

BEAM DYNAMICS IN A HIGH CURRENT SC PROTON LINAC FOR NUCLEAR WASTE TRANSMUTATION

G. Bellomo, P. Pierini,

INFN Milano - LASA, Via Fratelli Cervi, 201, I-20090 Segrate (MI), Italy

Abstract

INFN is studying a 100 MeV to 1.6 GeV high current (25 mA) proton linac for waste transmutation and energy production. The beam dynamics in the superconducting linac have been studied with multiparticle tracking codes. The results of this activity will be presented here, with a description of a simulation code that we are developing for space charge dominated beam dynamics.

1 THE LINAC DESIGN

INFN has started a two year program (TRASCO) for the design study and for R&D on components of a high power superconducting proton Linac for nuclear waste transmutation. The status of the program is reported in a separate contribution at this Conference [1].

The 352 MHz superconducting linac, operating at 25 mA in the energy range 100-1600 MeV, uses five cell elliptical cavities designed for synchronous β of 0.5, 0.65, 0.85. The rationale of this choice, based on the efficiency of the cavities, has already been presented in Ref. [2].

The peak energy gain in the cavities, at the nominal synchronous phase $\phi_s = -30$ deg, is 4, 6.5 and 10 MeV, respectively. The cryostats accommodate 2, 3 and 4 cavities in the three sections.

The transverse focusing is provided by a periodic array of quadrupole doublets, and the cavity cryostats are placed in the drift between the doublets. The lengths of the focusing periods are 8.0, 11.2 and 15.3 m.

The lattice parameters have been chosen so that the zero current phase advances in the first period of each section are close to 90 degrees and the tune depression is around 0.7.

The quadrupoles in each section have an almost constant gradient, so that the transverse phase advance is smoothly decreasing at approximately the same rate of the longitudinal phase advance.

The matching between sections is controlled with the gradient of the doublet at the interface and the tuning of the synchronous phases of the cavities close to the interface.

The rms beam sizes along the linac are shown in Figure 1. The input rms emittances are 0.4π mm mrad and 0.2π deg MeV.

Since the beam pipe radius is 100 mm the ratio between the aperture and the rms beam size is larger than 25 and reaches the value of 40 at the end of the linac.

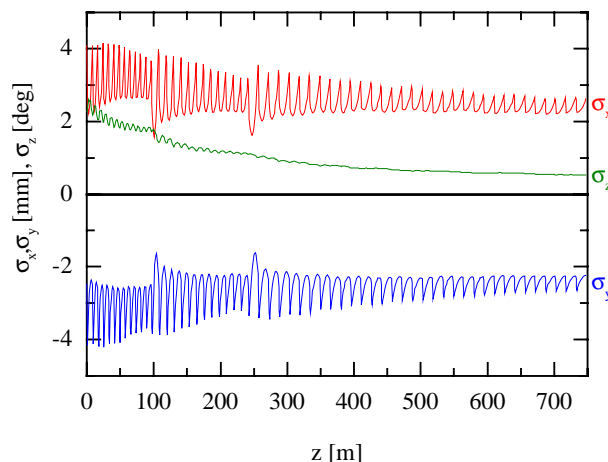


Figure 1: Rms beam sizes along the linac. On the positive ordinates: horizontal and longitudinal, On the negative ordinates: vertical.

2 MULTIPARTICLE SIMULATIONS

2.1 Initial results

Initial multiparticle tracking has been performed with a preliminary version of a code we are developing, using a limited number of particles (up to 5000) and space charge calculations via a direct point-to-point scheme. The results, reported at EPAC 98 [3], are summarized here.

For the rms emittances assumed in these simulations, 0.2π mm mrad and 0.2π deg MeV, an increase of 70% of the transverse rms emittances and a decrease of 40% longitudinal emittance was observed. The growth occurred mostly in the first linac section (100-200 MeV). Using as a guideline the equipartitioning criteria two alternatives were found to limit the emittance growth:

- a decrease of the period length of each section (this can be reached with 1, 2, 2 cavities per cryomodule in the sections, but results in a linac lengthening);
- an increase by a factor two of the transverse rms emittances. The beam sizes increase approximately by 50%, but the ratio aperture to rms is still larger than 20.

The latter solution, presented in Figure 1, has been chosen to be explored in more detail with the enhanced capabilities of the code, using up to 10^5 particles, and will be reported in the following subsection.

The first solution will be examined in the future, in connection with the foreseen increase of the current up to 50, or even 100 mA [1].

2.2 The multigrid code

A multiparticle beam dynamics code has been developed for the SC linac simulations. The particles are advanced through direct integration of the equations of motion along a beamline composed of quadrupoles, drift spaces and RF cavities.

The on-axis longitudinal field of the cavities is either assumed as an analytical expression for an ideal cavity or provided as an input. An iterative method to set the RF field phases of each cavity to the synchronous values, defined at the cavity center, has been implemented.

Space charge kicks are applied every few integration timesteps. A 3D space charge routine based on a fast multigrid[4] Poisson solver and a Cloud in Cell (CIC) charge assignment algorithm have been implemented in the code. The charge distribution is evaluated in the reference particle rest frame, using a CIC density smoothing algorithm. The Poisson equation for the electric potential is then solved on a square mesh (typically consisting of 33x33x33 points, extending at least to 6 rms) using a fast multigrid solver. The electric field in the rest frame is then computed from the potential, transformed to the laboratory frame and the corresponding kick, interpolated from the grid values, is applied to each particle of the beam.

Multigrid methods are surely among the fastest iterative methods for the solution of elliptic problems[4]. The model problem is represented on a series of coarser grids, obtained, for example, doubling the mesh size. Appropriate operators allow to “transport” the information (i.e. the source term, the residuals or an estimate of the solution) down one coarser grid level (“coarsening”) or up one finer grid level (“prolongation”). The approximate solutions at each grid level are then used to form a better solution of the problem on the finest. The approximate solutions at each grid level are obtained with a few cycles (2-4) of an ordinary relaxation method (here the Gauss-Seidel algorithm).

The multigrid scheme makes use of the smoothing properties of relaxation schemes: the high frequencies (relative to the grid in use) of the error decay very rapidly. This, together with the use of a hierarchy of coarser and coarser grids, allows a very effective improvement in the convergence with respect of a standard relaxation scheme on a single grid, which has to face a poor performance with the smooth components of the error. V-cycle multigrid schemes converge (to 10^{-6} in norm) in 4 to 6 iterations, independently from the grid size.

A further acceleration in the convergence to the required accuracy for the space charge fields in a beam dynamics code is the use of the potential map evaluated in the previous space charge step, in order to have a better initial guess for the unknown potential.

The multigrid Poisson solver has been employed for beam dynamics simulations with up to 10^5 particles for the 750 m TRASCO linac, as reported in the following.

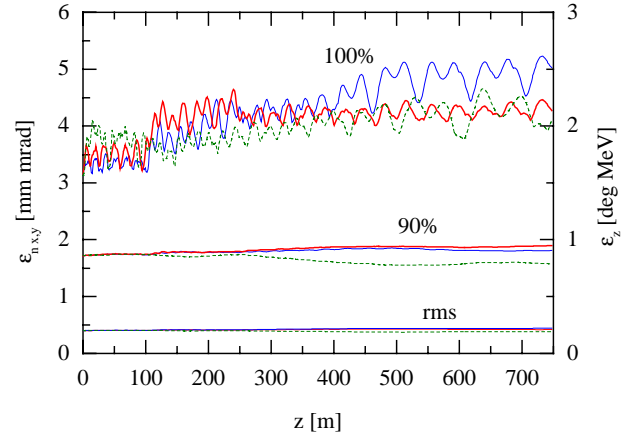


Figure 2: The rms, 90% and total (100%) normalized emittances along the linac. Solid curves (left axis): transverse emittances; dashed curve (right axis): longitudinal emittance. 10^5 particles in the simulation.

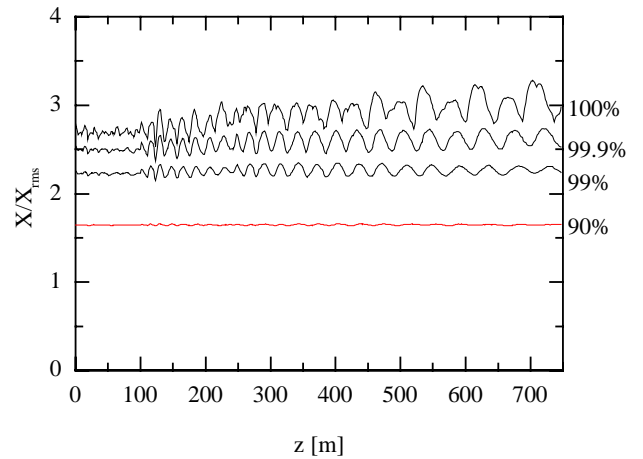


Figure 3: Ratio of the horizontal beam size to the rms value along the linac, for different beam fractions (10^5 particles in the simulation).

2.3 Matched beam case

The simulations with the multigrid code, using 10000 particles, have confirmed the results obtained with the point to point space charge routine. Simulations with 10^5 particles were then performed to explore in more details the tails of the beam distribution.

The simulations discussed here have been performed using a 6D waterbag distribution for the particle loading with a quiet random number generator [5]. However, more particle loading options still need to be implemented in the code, in particular the stationary distributions described in Ref. [6].

The input rms beam Twiss parameters and the matching conditions for the section transitions have been calculated with a linear space charge code [7].

The evolution of the rms, 90% and total emittances along the linac is plotted in Figure 2. The rms emittance growth is less than 10%.

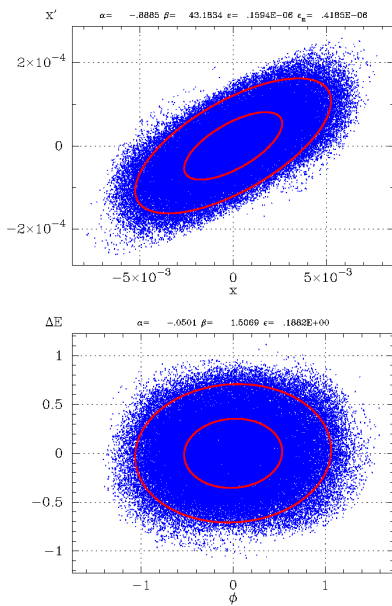


Figure 4: Transverse (upper) and longitudinal (lower) phase space projections at the end of the linac (1.6 GeV). Also plotted are the rms and the 90% beam ellipses. The simulation has been performed with 10^5 particles. Units are m, rad and deg, MeV.

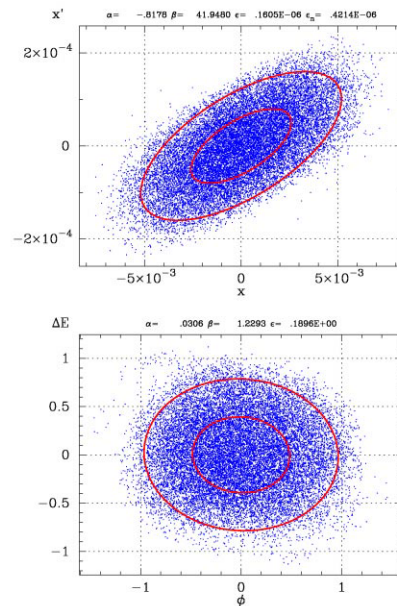


Figure 5: Transverse (upper) and longitudinal (lower) phase space projections at the end of the linac for an initial mismatched beam (10% in x,y and z). The simulation has been performed with 20000 particles. Units are m, rad and deg, MeV.

The increase of the total emittance is moderate (less than 50%), so that the ratio total/rms grows approximately from 8 to 12. The discontinuity at the interface between section 1 and section 2 (approximately at $z=100$ m) can be seen from Fig. 2.

The regular behavior of the beam is more apparent in Fig. 3, where we plot the ratio X/X_{rms} corresponding to various beam fractions. The 100% beam size is remarkably constant in the first linac section (up to $z=100$ m), indicating, in our opinion, a good matching of the beam distribution in the linac. In the second and third linac sections the betatron oscillation of the beam tails (99% and beyond) can be clearly seen, indicating a mismatch of the tails of the distribution. Similar plots can be shown for the vertical and longitudinal distributions.

A close examination of the phase space projections at the end of the beamline, see Fig. 4, show the formation of beam tails, in both the transverse and longitudinal planes. The deformation of the phase space is also evident looking at the beam fraction outside the 90% ellipses.

2.4 Initial beam mismatch

Simulations with a 10% mismatched initial beam (in a single plane and in all planes) have been performed with 20000 particles. No appreciable variations of the rms beam emittances have been observed. The total beam emittances increase by 20% with respect to the matched beam case, in agreement with similar calculations [8].

The phase space projections for a mismatch of +10% in the three planes are shown in Fig. 5; signs of filamentation in the longitudinal plane are barely visible.

3 CONCLUSIONS

The beam dynamics multiparticle simulations of the linac, using up to 10^5 particles, have shown a modest 10% increase of the rms emittances and a good behavior of the total beam sizes and distribution along the linac.

Initial calculations with mismatched input beams (10%, in one plane or in all planes) have shown a remarkable stability in the rms emittances, with no significant sign of halo development.

A revision of the linac design will be undertaken in the future to increase the current up to 50 mA and to explore the constraints imposed by the 100 mA operation.

4 REFERENCES

- [1] C. Pagani, D. Barni, G. Bellomo, R. Parodi, P. Pierini, paper TH4108 at this Conference.
- [2] C. Pagani, G. Bellomo, P. Pierini, G. Travish, D. Barni, A. Bosotti, R. Parodi, in Proceedings of the 1997 Part. Acc. Conf., Vancouver, Canada.
- [3] G. Bellomo, P. Pierini, in Proceedings of the 1998 European Part. Acc. Conference, Stockholm, Sweden.
- [4] W.L. Briggs, "A Multigrid Tutorial", SIAM, Philadelphia, Pennsylvania 1987.
- [5] J.M. Hammersley, D.C. Handscomb, "Montecarlo methods", (Methuen, London 1964).
- [6] A.V. Fedotov, R.L. Gluckstern, S.S. Kurennoy, R.D. Ryne, in Proceedings of the 1998 European Part. Acc. Conference, Stockholm, Sweden.
- [7] TRACE3-D, LANL Report LA-UR-90-4146 (1987).
- [8] M. Pabst et al, in Proceedings of the 1998 European Part. Acc. Conference, Stockholm, Sweden.